Optimal Power Allocation for Fading Channels in Cognitive Radio Networks: Ergodic Capacity and Outage Capacity

Xin Kang, *Student Member, IEEE*, Ying-Chang Liang, *Senior Member, IEEE*, Arumugam Nallanathan, *Senior Member, IEEE*, Hari Krishna Garg, *Senior Member, IEEE*, and Rui Zhang, *Member, IEEE*

***Abstract*—A cognitive radio network (CRN) is formed by either allowing the secondary users (SUs) in a secondary communication network (SCN) to opportunistically operate in the frequency bands originally allocated to a primary communication network (PCN) or by allowing SCN to coexist with the primary users (PUs) in PCN as long as the interference caused by SCN to each PU is properly regulated. In this paper, we consider the latter case, known as spectrum sharing, and study the optimal power allocation strategies to achieve the ergodic capacity and the outage capacity of the SU fading channel under different types of power constraints and fading channel models. In particular, besides the interference power constraint at PU, the transmit power constraint of SU is also considered. Since the transmit power and the interference power can be limited either by a peak or an average constraint, various combinations of power constraints are studied. It is shown that there is a capacity gain for SU under the average over the peak transmit/interference power constraint. It is also shown that fading for the channel between SU transmitter and PU receiver is usually a beneficial factor for enhancing the SU channel capacities.**

***Index Terms*—Cognitive radio, power control, ergodic capacity, outage capacity, delay-limited capacity, spectrum sharing, interference power constraint, fading channel.**

I. Introduction

RADIO spectrum is a precious and limited resource for wireless communication networks. With the emergence of new wireless applications, the currently deployed spectrum is becoming increasingly more crowded. Hence, how to accommodate more wireless services within the limited spectrum becomes a challenging problem. On the other hand, according to the report published by the Federal Communication Commission (FCC), most of the allocated spectrum today is under-utilized [1]. This fact indicates that it is perhaps the inefficient and inflexible spectrum allocation policy rather than the physical shortage of spectrum that causes the spectrum scarcity.

Cognitive radio (CR) [2] is a promising technology to deal with the spectrum under-utilization problem caused by the current inflexible spectrum allocation policy. In a cognitive radio network (CRN), a secondary user (SU) in the secondary communication network (SCN) is allowed to access the spectrum that is originally allocated to the primary users (PUs) when the spectrum is not used by any PU. This secondary spectrum usage method is called *opportunistic spectrum access* [3]. In this way, the spectrum utilization efficiency can be greatly improved. However, to precisely detect a vacant spectrum is not an easy task [4]. Alternatively, CRN can also be designed to allow simultaneous transmission of PUs and SUs. From PU's perspective, SU is allowed to transmit as long as the interference from SU does not degrade the quality of service (QoS) of PU to an unacceptable level. From SU's perspective, SU should control its transmit power properly in order to achieve a reasonably high transmission rate without causing too much interference to PU. This transmission strategy is termed as *spectrum sharing* [5]. Traditionally, the capacity of fading channels is studied under various transmit power constraints, and the corresponding optimal and suboptimal power allocation policies are given in, e.g., [6], [7], [8]. Recently, study on the channel capacity of SU link under spectrum sharing has attracted a lot of attention. Specifically, SU channel capacity under spectrum sharing was addressed by Gastpar in [9], where the capacities of different additive white Gaussian noise (AWGN) channels are derived under a received power constraint. The capacities derived in [9] are shown to be quite similar to those under a transmit power constraint. This is non-surprising because the ratio of the received power to the transmit power is fixed in an AWGN channel; thus, considering a received power constraint is equivalent to considering a transmit power constraint. However, in the presence of fading, the situation becomes quite different. In [5], the authors derived the optimal power allocation strategy for a SU coexisting with a PU subject to an interference power constraint at PU receiver, and evaluated the ergodic capacity for SU channel for different fading channel models. In [10], the authors considered the outage capacity under both the peak and the average interference power constraints. It is noted that optimal design of SU transmission strategy under interference-power constraints at PU receivers has also been studied in [11]

Manuscript received December 25, 2007; revised July 8, 2008; accepted August 21, 2008. The associate editor coordinating the review of this paper and approving it for publication was J. R. Luo.

X. Kang and H. K. Garg are with the Department of Electrical & Computer Engineering, National University of Singapore, 119260, Singapore (e-mail: {kangxin, eleghk}@nus.edu.sg).

Y.-C. Liang and R. Zhang are with the Institute for Infocomm Research, 1 Fusionopolis Way, ♯21-01 Connexis, South Tower, Singapore 138632 (e-mail: {ycliang, rzhang}@i2r.a-star.edu.sg).

A. Nallanathan is with the Division of Engineering, King's College London, London, United Kingdom (e-mail: nallanathan@ieee.org).

This work was supported by the National University of Singapore, Singapore under Grant R-263-000-436-112.

Digital Object Identifier 10.1109/TWC.2009.071448

for multi-antenna CR transmitters, and in [12] for multiple CR transmitters in a multiple-access channel (MAC).

In this paper, we study the ergodic capacity, the delay-limited capacity, and the outage capacity of SU block-fading (BF) channels under spectrum sharing. For a BF channel [13], [14], the channel remains constant during each transmission block, but possibly changes from one block to another. For BF channels, the ergodic capacity is defined as the maximum achievable rate averaged over all the fading blocks. Ergodic capacity is a good performance limit indicator for delay-insensitive services, when the codeword length can be sufficiently long to span over all the fading blocks. However, for real-time applications, it is more appropriate to consider the delay-limited capacity introduced in [15], which is defined as the maximum constant transmission rate achievable over each of the fading blocks. For certain severe fading scenarios, such as Rayleigh fading, however, the delay-limited capacity can be zero. Thus, for such scenarios, the outage capacity [13], [14], which is defined as the maximum constant rate that can be maintained over fading blocks with a given outage probability, will be a good choice.

In this paper, we derive the optimal power allocation strategies for SU to achieve aforementioned capacities. Besides the interference power constraint to protect PU, we also consider the transmit power constraint of SU transmitter. Since the transmit power and the interference power can be limited either by a peak or an average constraint, different combinations of power constraints are considered. It is shown that there is a capacity gain for SU under the average over the peak transmit/interference power constraint. Furthermore, we provide closed-form solutions for the delay-limited capacity and the outage probability under several typical channel fading models, including Rayleigh fading, Nakagami fading, and Log-normal fading. It is observed that fading for the channel between SU transmitter and PU receiver can be a beneficial factor for enhancing the SU channel capacities.

The rest of the paper is organized as follows. Section II describes the system model and presents various transmit and interference power constraints. Then, the ergodic capacity, the delay-limited capacity, and the outage capacity under different combinations of peak/average transmit and interference power constraints are studied in Section III, Section IV, and Section V, respectively. In Section VI, the simulation results are presented and discussed. Finally, Section VII concludes the paper.

Notation: $\mathrm{E}[\cdot]$ denotes the statistical expectation. K denotes the constant $\log_2 e$, where e is the base of natural logarithm. $\max(x, y)$ and $\min(x, y)$ denote the maximum and the minimum element between x and y, respectively. $(\cdot)^+$ stands for $\max(0, \cdot)$. The symbol $\triangleq$ means "defined as".

II. System Model and Power Constraints

A. System model

As illustrated in Fig. 1, we consider a spectrum sharing network with one PU and one SU. The link between SU transmitter (SU-Tx) and PU receiver (PU-Rx) is assumed to be a flat fading channel with instantaneous channel power gain g_0 and the AWGN n_0. SU channel between SU-Tx and SU receiver (SU-Rx) is also a flat fading channel characterized

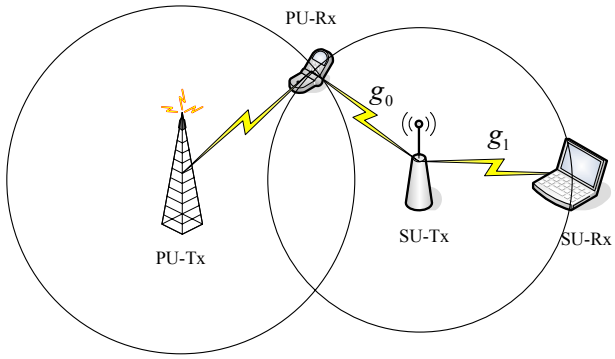

Fig. 1. System model for spectrum sharing in cognitive radio networks.

by instantaneous channel power gain g_1 and the AWGN n_1. The noises n_0 and n_1 are assumed to be independent random variables with the distribution $\mathcal{CN}(0, N_0)$ (circularly symmetric complex Gaussian variable with mean zero and variance N_0). The channel power gains, g_0 and g_1, are assumed to be ergodic and stationary with probability density function (PDF) $f_0(g_0)$, and $f_1(g_1)$, respectively. Perfect channel state information (CSI) on g_0 and g_1 is assumed to be available at SU-Tx. Furthermore, it is assumed that the interference from PU-Tx to SU-Rx can be ignored or considered in the AWGN at SU-Rx.

B. Power constraints

Previous study on the fading channel capacity usually assumes two types of power constraints at the transmitter: peak transmit power constraint and average transmit power constraint, either individually [14] or simultaneously [16]. The peak power limitation may be due to the nonlinearity of power amplifiers in practice, while the average power is restricted below a certain level to keep the long-term power budget. In this paper, we denote the instantaneous transmit power at SU-Tx for the channel gain pair (g_0, g_1) as $P(g_0, g_1)$, and obviously it follows

$$P(g_0, g_1) \geq 0, \forall (g_0, g_1). \tag{1}$$

Let P_{pk} be the peak transmit power limit and P_{av} be the average transmit power limit. The peak transmit power constraint can then be represented by

$$P(g_0, g_1) \leq P_{pk}, \forall (g_0, g_1), \tag{2}$$

and the average transmit power constraint can be represented by

$$\mathrm{E}[P(g_0, g_1)] \leq P_{av}. \tag{3}$$

On the other hand, motivated by the interference temperature concept in [3], researchers have investigated SU channel capacities with received power constraints. If PU provides delay-insensitive services, an average received power constraint can be used to guarantee a long-term QoS of PU. Let Q_{av} denote the average received power limit at PU-Rx. The average interference power constraint can then be written as

$$\mathrm{E}[g_0 P(g_0, g_1)] \leq Q_{av}. \tag{4}$$

If the service provided by PU has an instantaneous QoS requirement, the peak interference power constraint may be more appropriate. Let Q_{pk} denote the peak received power at the PU-Rx. The peak interference power constraint can then be written as

$$g_0 P(g_0, g_1) \leq Q_{pk}, \forall (g_0, g_1). \tag{5}$$

For the purpose of exposition, we combine the transmit power constraint with the interference power constraint, and obtain the following four sets of power constraints:

$$\mathscr{F}_1 \triangleq \{P(g_0, g_1) : (1), (2), (5)\}, \tag{6}$$

$$\mathscr{F}_2 \triangleq \{P(g_0, g_1) : (1), (2), (4)\}, \tag{7}$$

$$\mathscr{F}_3 \triangleq \{P(g_0, g_1) : (1), (3), (5)\}, \tag{8}$$

$$\mathscr{F}_4 \triangleq \{P(g_0, g_1) : (1), (3), (4)\}. \tag{9}$$

III. Ergodic Capacity

For BF channels, ergodic capacity is defined as the maximum achievable rate averaged over all the fading blocks. Using a similar approach as in [6], the ergodic capacity of the secondary link can be obtained by solving the following optimization problem,

$$\max_{P(g_0,g_1)\in\mathscr{F}} \mathrm{E}\left[\log_2\left(1 + \frac{g_1 P(g_0, g_1)}{N_0}\right)\right], \tag{10}$$

where $\mathscr{F} \in \{\mathscr{F}_1, \mathscr{F}_2, \mathscr{F}_3, \mathscr{F}_4\}$, and the expectation is taken over (g_0, g_1). In what follows, we will study (10) under $\mathscr{F}_1$, $\mathscr{F}_2$, $\mathscr{F}_3$, and $\mathscr{F}_4$, respectively.

A. Peak transmit power constraint and peak interference power constraint

In this case, $\mathscr{F}$ in (10) becomes $\mathscr{F}_1$. The two constraints in $\mathscr{F}_1$ can be combined as $P(g_0, g_1) \leq \min\{P_{pk}, \frac{Q_{pk}}{g_0}\}$. Therefore, the capacity is maximized by transmitting at the maximum instantaneous power expressed as

$$P(g_0, g_1) = \begin{cases} P_{pk}, & g_0 \leq \frac{Q_{pk}}{P_{pk}} \\ \frac{Q_{pk}}{g_0}, & \text{otherwise} \end{cases}. \tag{11}$$

From (11), it is observed that, when g_0 is less than a given threshold, SU-Tx can transmit at its maximum power, P_{pk}, which satisfies the interference power constraint at PU-Rx. This indicates that sufficiently severe fading of the channel between SU-Tx and PU-Rx is good from both viewpoints of protecting PU-Rx and maximizing SU throughput. However, when g_0 becomes larger than this threshold, SU-Tx transmits with decreasing power values that are inversely proportional to g_0.

B. Peak transmit power constraint and average interference power constraint

In this case, $\mathscr{F}$ in (10) becomes $\mathscr{F}_2$. The optimal power allocation is given by the following theorem.

Theorem 1: The optimal solution of (10) subject to the power constraints given in $\mathscr{F}_2$ is

$$P(g_0, g_1) = \begin{cases} 0, & g_0 \geq \frac{K g_1}{\lambda N_0} \\ \frac{K}{\lambda g_0} - \frac{N_0}{g_1}, & \frac{K g_1}{\lambda N_0} > g_0 > \frac{K}{\lambda(P_{pk} + \frac{N_0}{g_1})} \\ P_{pk}, & g_0 \leq \frac{K}{\lambda(P_{pk} + \frac{N_0}{g_1})} \end{cases}, \tag{12}$$

where λ is the nonnegative dual variable associated with (4) in $\mathscr{F}_2$. If (4) in $\mathscr{F}_2$ is satisfied with strict inequality, λ must be zero. Otherwise, λ can be obtained by substituting (12) into the constraint $\mathrm{E}[g_0 P(g_0, g_1)] = Q_{av}$.

Proof: See Appendix A. ■

As can be seen from (12), if P_{pk} is sufficiently large, the power allocation scheme reduces to that in [5], where the ergodic capacity of fading channels is studied under the interference power constraint only. It is also noticed that the power allocation scheme given by (12) has the same structure as that in [16], where the ergodic capacity of fading channels is studied under both peak and average transmit power constraints. The main difference is that the power allocation scheme given by (12) is not only related to SU channel but also related to the channel between SU-Tx and PU-Rx.

C. Average transmit power constraint and peak interference power constraint

In this case, $\mathscr{F}$ in (10) becomes $\mathscr{F}_3$. The optimal power allocation of this problem is given by the following theorem.

Theorem 2: The optimal solution of (10) subject to the constraints given in $\mathscr{F}_3$ is

$$P(g_0, g_1) = \begin{cases} 0, & g_1 \leq \frac{\lambda N_0}{K} \\ \frac{K}{\lambda} - \frac{N_0}{g_1}, & g_1 > \frac{\lambda N_0}{K}, g_0 < \frac{Q_{pk}}{(\frac{K}{\lambda} - \frac{N_0}{g_1})} \\ \frac{Q_{pk}}{g_0}, & g_1 > \frac{\lambda N_0}{K}, g_0 \geq \frac{Q_{pk}}{(\frac{K}{\lambda} - \frac{N_0}{g_1})} \end{cases}, \tag{13}$$

where λ is the nonnegative dual variable associated with (3) in $\mathscr{F}_3$. If (3) in $\mathscr{F}_3$ is satisfied with strict inequality, λ must be zero. Otherwise, λ can be obtained by substituting (13) into the constraint $\mathrm{E}[P(g_0, g_1)] = P_{av}$.

Theorem 2 can be proved similarly as Theorem 1, we thus omit the details here for brevity.

From (13), it is seen that, when the channel between SU-Tx and PU-Rx experiences sufficiently severe fading or Q_{pk} is sufficiently large, the power allocation reduces to the conventional water-filling solution [6]. It is also observed that the power allocation given in (13) is capped by $\frac{Q_{pk}}{g_0}$, and this cap increases with decreasing g_0. This indicates that fading for the channel between SU-Tx and PU-Rx enables SU-Tx to transmit more power under the same value of Q_{pk}.

D. Average transmit power constraint and average interference power constraint

In this case, $\mathscr{F}$ in (10) becomes $\mathscr{F}_4$. The optimal solution for this problem can be obtained by applying similar techniques as for Theorem 1, which can be expressed as

$$P(g_0, g_1) = \left(\frac{K}{\lambda + \mu g_0} - \frac{N_0}{g_1}\right)^+, \tag{14}$$

where λ and μ are the nonnegative dual variables associated with (3) and (4) in $\mathscr{F}_4$, respectively. If (3) or (4) in $\mathscr{F}_4$ is satisfied with strict inequality, λ or μ must be zero correspondingly. Otherwise, λ and μ can be jointly determined by substituting (14) into the constraints $\mathrm{E}[P(g_0, g_1)] = P_{av}$ and $\mathrm{E}[g_0 P(g_0, g_1)] = Q_{av}$.

IV. Delay-limited Capacity

For BF channels, delay-limited capacity [15] is defined as the maximum constant transmission rate achievable over each of the fading blocks. This is a good performance limit indicator for delay-sensitive services, which may require a constant rate transmission over all the fading blocks. Thus, the objective is to maximize such constant rate by adapting the transmit power of SU-Tx. At the same time, due to the coexistence with PU, the received interference power at the PU-Rx should not exceed the given threshold. In this section, the delay-limited capacity is studied under $\mathscr{F}_4$ only. This is due to the fact that delay-limited capacity can be shown to be zero under the other three combinations of power constraints for realistic fading channel models. Therefore, the delay-limited capacity can be obtained by solving the following problem:

$$\max_{P(g_0,g_1)\in\mathscr{F}_4} \log_2(1+\gamma), \tag{15}$$

$$\text{s. t.} \quad \frac{g_1 P(g_0,g_1)}{N_0} = \gamma, \ \forall (g_0,g_1). \tag{16}$$

where γ is the constant received signal-to-noise ratio (SNR) at SU-Rx for all pairs of (g_0, g_1).

Obviously, the delay-limited capacity is achieved when γ takes its maximum value. Therefore, the above problem is equivalent to finding the maximum value of γ under the power constraints in $\mathscr{F}_4$. From (16), we have $P(g_0,g_1) = \frac{\gamma N_0}{g_1}$. Substituting this into the power constraints given in $\mathscr{F}_4$ yields $\gamma \le \frac{P_{av}}{N_0 \mathrm{E}\left[\frac{1}{g_1}\right]}$ and $\gamma \le \frac{Q_{av}}{N_0 \mathrm{E}\left[\frac{g_0}{g_1}\right]}$, $\forall (g_0,g_1)$. Therefore, $\gamma_{max} = \min\left\{\frac{P_{av}}{N_0 \mathrm{E}\left[\frac{1}{g_1}\right]}, \frac{Q_{av}}{N_0 \mathrm{E}\left[\frac{g_0}{g_1}\right]}\right\}$. The delay-limited capacity is thus given by

$$C_d = \min\left\{\log_2\left(1+\frac{P_{av}}{N_0 \mathrm{E}\left[\frac{1}{g_1}\right]}\right), \log_2\left(1+\frac{Q_{av}}{N_0 \mathrm{E}\left[\frac{g_0}{g_1}\right]}\right)\right\}. \tag{17}$$

By setting $Q_{av} = +\infty$ in (17), it is easy to obtain the delay-limited capacity for the conventional fading channels [14]. Similarly, by setting $P_{av} = +\infty$, the delay-limited capacity under the interference power constraint only is obtained.

In the following, the delay-limited capacity is evaluated under different fading channel models.

A. Rayleigh fading

For Rayleigh fading, the channel power gains g_0 and g_1 are exponentially distributed. Assume g_0 and g_1 are unit-mean and mutually independent. Then, $\mathrm{E}\left[\frac{1}{g_1}\right]$ can be evaluated equal to $+\infty$. Furthermore, the PDF of $\frac{g_0}{g_1}$ is expressed as [5]

$$f_{\frac{g_0}{g_1}}(x) = \frac{1}{(x+1)^2}, \ x \ge 0. \tag{18}$$

Hence, $\mathrm{E}\left[\frac{g_0}{g_1}\right]$ can be shown to be $+\infty$. Therefore, from (17), the delay-limited capacity is zero for Rayleigh fading channels.

B. Nakagami fading

Another widely used channel model is Nakagami-m fading. For a unit-mean Nakagami fading channel, the distribution of channel power gain follows the Gamma distribution, which is expressed as

$$f_g(x) = \frac{m^m x^{(m-1)}}{\Gamma(m)} e^{-mx}, \ x \ge 0, \tag{19}$$

where $\Gamma(\cdot)$ is the Gamma function defined as $\Gamma(x) = \int_0^\infty t^{(x-1)} e^{-t} dt$, and m $(m \ge 1)$ is the ratio of the line-of-sight (LOS) signal power to that of the multi-path component. Then, by [17], $\mathrm{E}\left[\frac{1}{g_1}\right]$ is evaluated to be 1. If g_0 and g_1 are independent and have the same parameter m, the PDF of $\frac{g_0}{g_1}$ is [18]

$$f_{\frac{g_0}{g_1}}(x) = \frac{x^{m-1}}{\mathcal{B}(m,m)(x+1)^{2m}}, \ x \ge 0, \tag{20}$$

where $\mathcal{B}(a,b)$ is the Beta function defined as $\mathcal{B}(a,b) = \frac{\Gamma(a)\Gamma(b)}{\Gamma(a+b)}$. Then $\mathrm{E}\left[\frac{g_0}{g_1}\right]$ can be evaluated equal to $\frac{m}{m-1}$. Hence, the delay-limited capacity in (17) is obtained as

$$C_d = \min\left\{\log_2\left(1+\frac{P_{av}}{N_0}\right), \log_2\left(1+\frac{Q_{av}}{N_0 \frac{m}{m-1}}\right)\right\}. \tag{21}$$

By setting $P_{av} = +\infty$, the delay-limited capacity under the interference power constraint only is obtained as $C_d = \log_2\left(1+\frac{Q_{av}}{N_0 \frac{m}{m-1}}\right)$. Furthermore, it is seen from (21) that the delay-limited capacity is determined by only the interference power constraint when $P_{av} \ge \frac{m-1}{m} Q_{av}$.

C. Log-normal shadowing

In the log-normal fading environment, the channel power gain is modeled by a log-normal random variable (r.v.) e^X where X is a zero-mean Gaussian r.v. with variance σ^2. In this case, we model the channel by letting $g_0 = e^{X_0}$ and $g_1 = e^{X_1}$, where X_0 and X_1 are independently distributed with mean zero and variance σ^2. Under the above assumptions, $g_0/g_1 = e^Y$ is also log-normally distributed with $Y = X_0 - X_1$ being Gaussian distributed with mean zero and variance $2\sigma^2$ [19]. In this case, $\mathrm{E}[\frac{1}{g_1}]$ and $\mathrm{E}[\frac{g_0}{g_1}]$ are evaluated to be $e^{\frac{\sigma^2}{2}}$ and e^{σ^2}, respectively. Hence, the delay-limited capacity in (17) is given by

$$C_d = \min\left\{\log_2\left(1+\frac{P_{av}}{N_0 e^{\frac{\sigma^2}{2}}}\right), \log_2\left(1+\frac{Q_{av}}{N_0 e^{\sigma^2}}\right)\right\}. \tag{22}$$

By setting $P_{av} = +\infty$, the delay-limited capacity under the interference power constraint only is obtained as $C_d = \log_2\left(1+\frac{Q_{av}}{N_0 e^{\sigma^2}}\right)$. Furthermore, it is seen from (22) that the delay-limited capacity will not be affected by the transmit power constraint when $P_{av} \ge e^{-\frac{\sigma^2}{2}} Q_{av}$.

V. Outage Capacity

For BF channels, outage capacity is defined as the maximum rate that can be maintained over the fading blocks with a given outage probability. Mathematically, this problem is defined as finding the optimal power allocation to achieve the maximum rate for a given outage probability, which is equivalent to

minimizing the outage probability for a given transmission rate (outage capacity) r_0, expressed as

$$\min_{P(g_0,g_1)\in\mathscr{F}} \quad Pr\left\{\log_2\left(1+\frac{g_1P(g_0,g_1)}{N_0}\right)<r_0\right\}, \quad (23)$$

where $Pr\{\cdot\}$ denotes the probability.

In the following, we will study the problem (23) under $\mathscr{F}_1$, $\mathscr{F}_2$, $\mathscr{F}_3$, and $\mathscr{F}_4$, respectively.

A. Peak transmit power constraint and peak interference power constraint

In this case, $\mathscr{F}$ in (23) becomes $\mathscr{F}_1$. The optimal solution of this problem can be easily obtained as

$$P(g_0,g_1)=\begin{cases}\frac{N_0(2^{r_0}-1)}{g_1}, & g_1\geq\frac{N_0(2^{r_0}-1)}{P_{pk}}, g_0\leq\frac{g_1Q_{pk}}{N_0(2^{r_0}-1)}\\ 0, & \text{otherwise}\end{cases}. \quad (24)$$

Substituting (24) into (23), we get

$$\mathscr{P}_{out}=1-\int_{\frac{N_0(2^{r_0}-1)}{P_{pk}}}^{+\infty}\int_0^{\frac{g_1Q_{pk}}{N_0(2^{r_0}-1)}} f_0(g_0)f_1(g_1)dg_0dg_1. \quad (25)$$

It is seen that (24) has the similar structure as the truncated channel inversion [6] for the convenional fading channel. The difference between these two methods lies in that the condition in (24) for channel inversion is determined by both g_0 and g_1, while that in [6] is by g_1 only. Therefore, we refer to this power allocation strategy as *two-dimensional-truncated-channel-inversion (2D-TCI)* over g_0 and g_1.

B. Peak transmit power constraint and average interference power constraint

In this case, $\mathscr{F}$ in (23) becomes $\mathscr{F}_2$. The optimal solution of this problem is given by the following theorem.

Theorem 3: The optimal solution of (23) subject to the power constraints given in $\mathscr{F}_2$ is

$$P(g_0,g_1)=\begin{cases}\frac{N_0(2^{r_0}-1)}{g_1}, & g_1\geq\frac{N_0(2^{r_0}-1)}{P_{pk}}, g_0<\frac{g_1}{\lambda N_0(2^{r_0}-1)}\\ 0, & \text{otherwise}\end{cases}, \quad (26)$$

and the corresponding minimum outage probability is given by

$$\mathscr{P}_{out}=1-\int_{\frac{N_0(2^{r_0}-1)}{P_{pk}}}^{+\infty}\int_0^{\frac{g_1}{\lambda N_0(2^{r_0}-1)}} f_0(g_0)f_1(g_1)dg_0dg_1, \quad (27)$$

where λ is the nonnegative dual variable associated with (4) in $\mathscr{F}_2$. If (4) in $\mathscr{F}_2$ is satisfied with strict inequality, λ must be zero. Otherwise, λ can be obtained by substituting (26) into the constraint $\mathrm{E}[g_0P(g_0,g_1)]=Q_{av}$.

Proof: See Appendix B. ∎

It is seen that (26) has the same structure as that in (24). Therefore, the optimal power control policy obtained in (26) is also 2D-TCI.

C. Average transmit power constraint and peak interference power constraint

In this case, $\mathscr{F}$ in (23) becomes $\mathscr{F}_3$. The optimal solution of this problem is given by the following theorem.

Theorem 4: The optimal solution of (23) subject to the power constraints given in $\mathscr{F}_3$ is

$$P(g_0,g_1)=\begin{cases}\frac{N_0(2^{r_0}-1)}{g_1}, & g_1>\lambda N_0(2^{r_0}-1), g_0\leq\frac{g_1Q_{pk}}{N_0(2^{r_0}-1)}\\ 0, & \text{otherwise}\end{cases}, \quad (28)$$

and the corresponding minimum outage probability is given by

$$\mathscr{P}_{out}=1-\int_{\lambda N_0(2^{r_0}-1)}^{+\infty}\int_0^{\frac{g_1Q_{pk}}{N_0(2^{r_0}-1)}} f_0(g_0)f_1(g_1)dg_0dg_1, \quad (29)$$

where λ is the nonnegative dual variable associated with (3) in $\mathscr{F}_3$. If (3) in $\mathscr{F}_3$ is satisfied with strict inequality, λ must be zero. Otherwise, λ can be obtained by substituting (28) into the constraint $\mathrm{E}[P(g_0,g_1)]=P_{av}$,

Theorem 4 can be proved similarly as Theorem 3; the proof is thus omitted here. Clearly, the power control policy given in (28) is also 2D-TCI.

D. Average transmit power constraint and average interference power constraint

In this case, $\mathscr{F}$ in (23) becomes $\mathscr{F}_4$. The optimal solution of (23) in this case is given by the following theorem.

Theorem 5: The optimal solution of (23) subject to the power constraints given in $\mathscr{F}_4$ is

$$P(g_0,g_1)=\begin{cases}\frac{N_0(2^{r_0}-1)}{g_1}, & \lambda+\mu g_0<\frac{g_1}{N_0(2^{r_0}-1)}\\ 0, & \text{otherwise}\end{cases}, \quad (30)$$

where λ and μ are the nonnegative dual variables associated with (3) and (4) in $\mathscr{F}_4$, respectively. If (3) or (4) in $\mathscr{F}_4$ is satisfied with strict inequality, λ or μ must be zero correspondingly. Otherwise, λ and μ can be jointly determined by substituting (30) into the constraints $\mathrm{E}[P(g_0,g_1)]=P_{av}$ and $\mathrm{E}[g_0P(g_0,g_1)]=Q_{av}$.

Theorem 5 can be proved similarly as Theorem 3.

E. Analytical Results

In this part, we provide the analytical results for the minimum outage probability under only the peak or the average interference power constraint.

1) Peak interference power constraint only: From (24), by setting $P_{pk}=+\infty$, we have

$$P(g_0,g_1)=\frac{Q_{pk}}{g_0}. \quad (31)$$

Substituting (31) into (23) yields

$$\mathscr{P}_{out}=Pr\left\{\frac{g_1}{g_0}<\frac{N_0(2^{r_0}-1)}{Q_{pk}}\right\}. \quad (32)$$

In the following, the minimum outage probability is evaluated under different fading models.

a) Rayleigh fading: Since $\frac{g_1}{g_0}$ has the same PDF as $\frac{g_0}{g_1}$, with the PDF of $\frac{g_0}{g_1}$ given in (18), we have

$$\mathscr{P}_{out}=\int_0^{\frac{N_0(2^{r_0}-1)}{Q_{pk}}}\frac{1}{(x+1)^2}dx=1-\frac{Q_{pk}}{N_0\left(2^{r_0}-1\right)+Q_{pk}}. \quad (33)$$

b) Nakagami fading: With the PDF of $\frac{g_1}{g_0}$ given in (20) (note that $\frac{g_1}{g_0}$ has the same PDF as $\frac{g_0}{g_1}$), we have

$$\begin{aligned}\mathscr{P}_{out} &= \int_0^{\frac{N_0(2^{r_0}-1)}{Q_{pk}}}\frac{x^{m-1}}{\mathcal{B}(m,m)(x+1)^{2m}}dx \\ &= \frac{1}{\mathcal{B}(m,m)}\int_0^{\frac{N_0(2^{r_0}-1)}{Q_{pk}}}\frac{x^{m-1}}{(x+1)^{2m}}dx. \end{aligned} \quad (34)$$

From (3.194-1) in [17], the above equation is simplified as

$$\begin{aligned}\mathscr{P}_{out} &= \frac{1}{m\mathcal{B}(m,m)}\left[\frac{N_0\left(2^{r_0}-1\right)}{Q_{pk}}\right]^m \\ &\quad\times\left\{{}_2F_1\left(2m,m;m+1;-\frac{N_0\left(2^{r_0}-1\right)}{Q_{pk}}\right)\right\}, \end{aligned} \quad (35)$$

where ${}_2F_1(a,b;c;x)$ is known as Gauss's hypergeometric function [17].

c) Log-normal fading: With the PDF of $\frac{g_1}{g_0}$ given in Section IV (note that $\frac{g_1}{g_0}$ has the same PDF as $\frac{g_0}{g_1}$), we have

$$\begin{aligned}\mathscr{P}_{out} &= Pr\left\{e^Y<\frac{N_0\left(2^{r_0}-1\right)}{Q_{pk}}\right\} \\ &= 1-\frac{1}{2}\mathrm{erfc}\left(\frac{1}{2\sigma}\log\left[\frac{N_0\left(2^{r_0}-1\right)}{Q_{pk}}\right]\right), \end{aligned} \quad (36)$$

where $\mathrm{erfc}(\cdot)$ is defined as $\mathrm{erfc}(t)\triangleq\frac{2}{\sqrt{\pi}}\int_t^\infty e^{-x^2}dx$.

2) Average interference power constraint only: From (26), by setting $P_{pk}=+\infty$ and denoting $\omega^*=\frac{1}{\lambda N_0(2^{r_0}-1)}$, we have

$$P(g_0,g_1)=\begin{cases}\frac{N_0(2^{r_0}-1)}{g_1}, & \frac{g_0}{g_1}<\omega^* \\ 0, & \text{otherwise}\end{cases}, \quad (37)$$

and the minimum outage probability is given by

$$\mathscr{P}_{out}=1-Pr\left\{\frac{g_0}{g_1}<\omega^*\right\}, \quad (38)$$

where ω^* is obtained by substituting (37) into the constraint $\mathrm{E}[g_0P(g_0,g_1)]=Q_{av}$.

In the following, the minimum outage probability is evaluated under different fading models.

a) Rayleigh fading: With the PDF of $\frac{g_0}{g_1}$ given in (18), we have

$$\mathscr{P}_{out}=1-\int_0^{\omega^*}\frac{1}{(x+1)^2}dx=\frac{1}{1+\omega^*}, \quad (39)$$

where ω^* is given by

$$\int_0^{\omega^*}\frac{x}{(x+1)^2}dx=\frac{Q_{av}}{N_0\left(2^{r_0}-1\right)}. \quad (40)$$

From (40), we have

$$\omega^*=\exp\left[\mathcal{W}\left(-\mathrm{e}^{-1-\frac{Q_{av}}{N_0(2^{r_0}-1)}}\right)+1+\frac{Q_{av}}{N_0\left(2^{r_0}-1\right)}\right]-1, \quad (41)$$

where $\mathcal{W}(x)$ is the Lambert-W function, which is defined as the inverse function of $f(w)=we^w$.

As can be seen from (39), if ω^* goes to infinity, the outage probability becomes zero; however, from (41), it is seen that ω^* is infinity only when $r_0=0$. This indicates that the zero-outage capacity for Rayleigh fading is zero, which is consistent with the result obtained in Section IV.

b) Nakagami fading: With the PDF of $\frac{g_0}{g_1}$ given in (20), we have

$$\begin{aligned}\mathscr{P}_{out} &= 1-\int_0^{\omega^*}\frac{x^{m-1}}{\mathcal{B}(m,m)(x+1)^{2m}}dx \\ &= 1-\frac{(\omega^*)^m}{m\mathcal{B}(m,m)}{}_2F_1\left(2m,m;m+1;-\omega^*\right), \end{aligned} \quad (42)$$

where ω^* is given by

$$\frac{1}{\mathcal{B}(m,m)}\int_0^{\omega^*}\frac{x^m}{(x+1)^{2m}}dx=\frac{Q_{av}}{N_0\left(2^{r_0}-1\right)}. \quad (43)$$

From (3.194-1) in [17], the above equation is simplified as

$$\frac{(w^*)^{m+1}\,{}_2F_1\left(2m,m+1;m+2;-w^*\right)}{(m+1)\mathcal{B}(m,m)}=\frac{Q_{av}}{N_0\left(2^{r_0}-1\right)}. \quad (44)$$

From the above, for the case of $m=2$, the outage probability can be shown to be $\mathscr{P}_{out}=\frac{1+3\omega^*}{(1+\omega^*)^3}$, and ω^* satisfies $2\left[1-\frac{1+3\omega^*+3(\omega^*)^2}{(1+\omega^*)^3}\right]=\frac{Q_{av}}{N_0(2^{r_0}-1)}$. From the above two formulas, when ω^* is infinity, the outage probability becomes zero and r_0 becomes the delay-limited capacity $\log_2\left(1+\frac{Q_{av}}{2N_0}\right)$. This is consistent with the result obtained in Section IV.

c) Log-normal fading: With the PDF of $\frac{g_0}{g_1}$ given in Section IV, we have

$$\mathscr{P}_{out}=1-Pr\left\{e^Y<\omega^*\right\}=\frac{1}{2}\mathrm{erfc}\left(\frac{1}{2\sigma}\log\left(\omega^*\right)\right), \quad (45)$$

where ω^* is determined by

$$\int_{-\infty}^{\log(\omega^*)}e^y\frac{1}{\sqrt{2\pi}\left(\sqrt{2}\sigma\right)}\exp\left(-\frac{y^2}{2\times2\sigma^2}\right)dy=\frac{Q_{av}}{N_0\left(2^{r_0}-1\right)}. \quad (46)$$

The above equation can be simplified to

$$e^{\sigma^2}\left[1-\frac{1}{2}\mathrm{erfc}\left(\frac{\log\left(\omega^*\right)-2\sigma^2}{2\sigma}\right)\right]=\frac{Q_{av}}{N_0\left(2^{r_0}-1\right)}. \quad (47)$$

It is seen from (45), the zero-outage probability is achieved when ω^* goes to infinity. It is clear from (47) that, when ω^* goes to infinity, $r_0=\log_2\left(1+\frac{Q_{av}}{N_0e^{\sigma^2}}\right)$. Again, this is consistent with the delay-limited capacity obtained in Section IV.

VI. Simulation Results

In this section, we present and discuss the simulation results for the capacities of the SU fading channels under spectrum sharing with the proposed power allocation strategies.

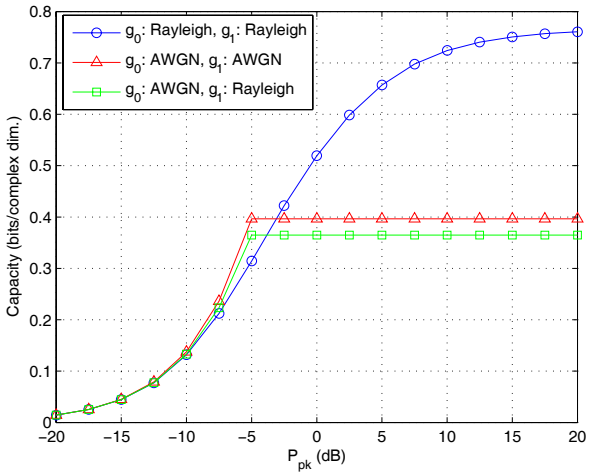

Fig. 2. Ergodic capacity vs. P_{pk} with $Q_{pk} = -5dB$ for different channel models.

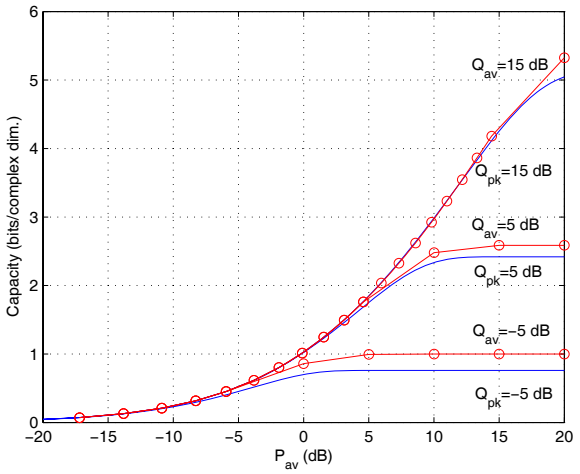

Fig. 4. Ergodic capacity vs. P_{av} under peak or average interference power constraints.

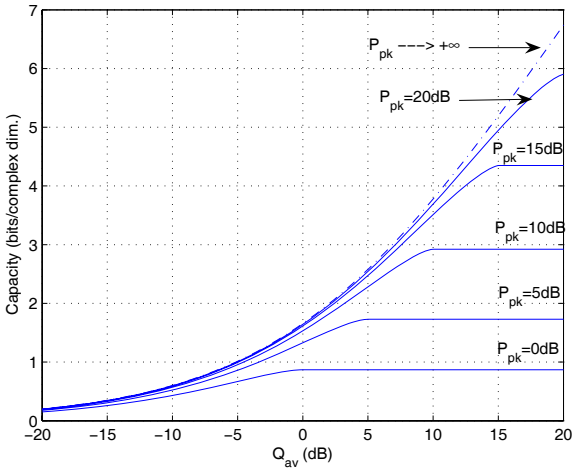

Fig. 3. Ergodic capacity under peak transmit and average interference power constraints.

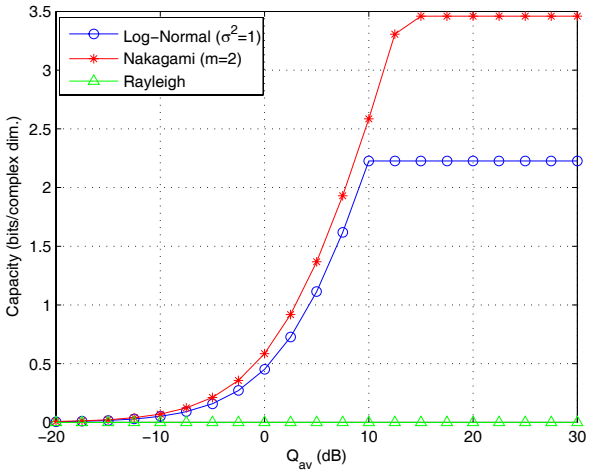

Fig. 5. Delay-limited capacity vs. Q_{av} with $P_{av} = 10dB$ for different fading channel models.

A. Ergodic capacity

In this subsection, the simulation results for ergodic capacity are presented. For Rayleigh fading channels, the channel power gains (exponentially distributed) are assumed to be unit mean. For AWGN channels, the channel power gains are also assumed to be one.

Fig. 2 shows the ergodic capacity under peak transmit and peak interference power constraints for $Q_{pk} = -5dB$. It is observed that when P_{pk} is very small, the ergodic capacities for the three curves shown in this figure are almost the same. This indicates that P_{pk} limits the performance of the network. However, when P_{pk} is sufficiently large compared with Q_{pk}, the ergodic capacities become different. In this case, when g_0 models the AWGN channel, the capacity of SU link when g_1 also models the AWGN channel is higher than that when g_1 models the Rayleigh fading channel. This indicates that fading of the SU channel is harmful. However, when g_1 models the Rayleigh fading channel, the capacity for SU link when g_0 models the AWGN channel is lower than that when g_0 models the Rayleigh fading channel. This illustrates that fading of the channel between SU-Tx and PU-Rx is a beneficial factor in terms of maximizing the ergodic capacity of SU channel.

Fig. 3 shows the ergodic capacity versus Q_{av} under peak transmit and average interference power constraints. For comparison, the curve with $P_{pk} = +\infty$ (i.e. no transmit power constraint) is also shown. It is observed that when Q_{av} is small, the capacities for different P_{pk}'s do not vary much. This illustrates that Q_{av} limits the achievable rate of SU. However, when P_{pk} is sufficiently large compared to Q_{av}, the capacities become flat. This indicates that P_{pk} becomes the dominant constraint in this case. Furthermore, with P_{pk} being sufficiently large, the ergodic capacity of SU channel becomes close to that without transmit power constraint.

Fig. 4 shows the ergodic capacity versus P_{av} under different types of interference power constraints. As shown in the figure, the ergodic capacity under average interference power constraint is larger than that under peak interference power constraint with the same value of P_{av}. This is because the power control of SU is more flexible under average over peak interference power constraint.

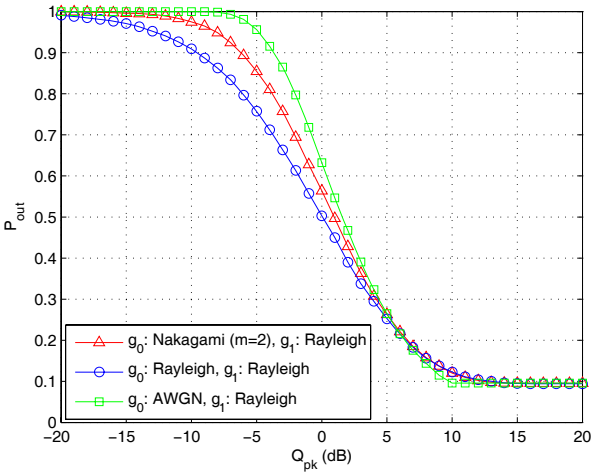

Fig. 6. Outage probability vs. Q_{pk} for $r_0 = 1$ bit/complex dim. $P_{pk} = 10dB$ for different fading channel models.

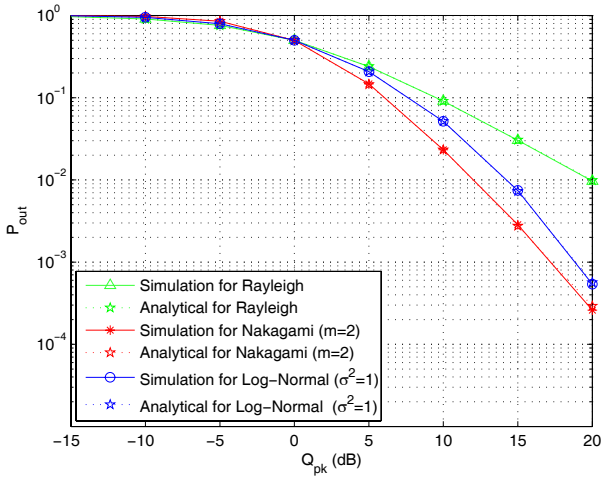

Fig. 8. Outage probability for $r_0 = 1$ bit/complex dim. under peak interference power constraint only.

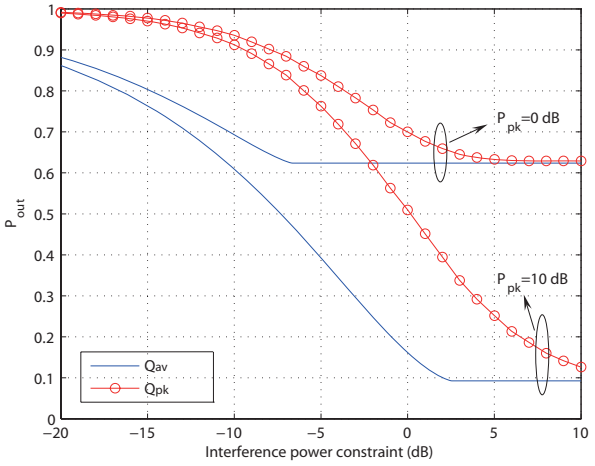

Fig. 7. Outage probability for $r_0 = 1$ bit/complex dim. under peak or average interference power constraints

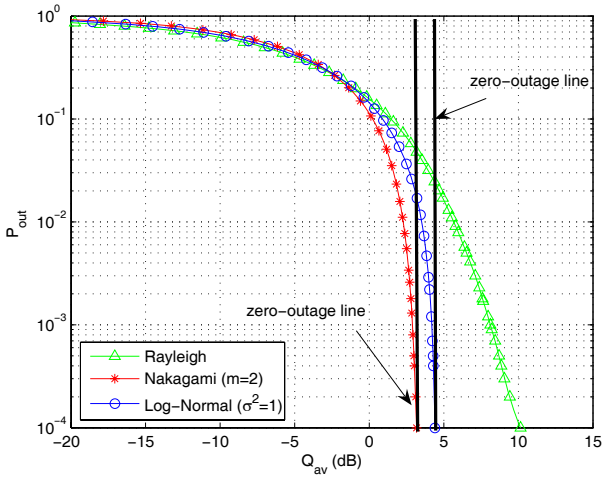

Fig. 9. Outage probability for $r_0 = 1$ bit/complex dim. under average interference power constraint only.

B. Delay-limited capacity and outage capacity

In this subsection, the simulation results for delay-limited and outage capacities are presented. For Rayleigh fading channels, the channel power gains (exponentially distributed) are assumed to be unit mean. Besides, $m = 2$ is chosen for the unit-mean Nakagami fading channels used in the simulation. For log-normal fading channels, $\sigma^2 = 1$ is used. This is because log-normal shadowing is usually characterized in terms of its dB-spread σ_{dB}, which ranges from $4dB$ to $12dB$ by empirical measurements, and is related to σ by $\sigma = 0.1\log(10)\sigma_{dB}$ [5]. We thus choose $\sigma^2 = 1$ as this value of σ makes the dB-spread lying within its typical ranges.

Fig. 5 shows the delay-limited capacity under $P_{av} = 10dB$ for different fading models versus Q_{av}. It is seen that the delay-limited capacity for Nakagami fading and log-normal shadowing increases with Q_{av}. However, when Q_{av} is sufficiently large, the delay-limited capacity will get saturated due to P_{av}. Note that the delay-limited capacity of Rayleigh fading model is zero regardless of Q_{av}. This is consistent with our analysis in Section IV.

Fig. 6 shows the outage probability for different fading models under $P_{pk} = 10dB$ and $r_0 = 1$ bit/complex dimension (dim.). It is seen that when Q_{pk} is small, the outage probability of SU link when g_0 models a fading channel is smaller than that when g_0 models the AWGN channel. Besides, more severe the fading is, the smaller the outage probability is. This illustrates that fading of the channel between SU-Tx and PU-Rx is good in terms of minimizing the outage probability of SU channel. However, when Q_{pk} has the same value of P_{pk}, the outage probability when g_0 models a fading channel is larger than that when g_0 models the AWGN channel. This can be foreseen from (24). When $Q_{pk} = P_{pk}$, the channel inversion condition for the AWGN case is $\frac{2^{r_0}-1}{g_1} \leq P_{pk}$. However, the channel inversion condition for the fading case is $\frac{2^{r_0}-1}{g_1} \leq \min(P_{pk}, \frac{Q_{pk}}{g_0})$, which can be more restrictive than that in the AWGN case if $g_0 > 1$. The higher the probability $g_0 > 1$ is, the larger the resultant outage probability is. However, when Q_{pk} is sufficiently large, both fading and AWGN channels will have the same outage probability, since

P_{pk} becomes the dominant constraint in this case.

Fig. 7 shows the outage probability under peak and average interference power constraints for $r_0 = 1$ bit/complex dim. under $P_{pk} = 0dB$ or $P_{pk} = 10dB$. It is seen that under the same P_{pk}, the outage probability under the average interference power constraint is smaller than that under the peak interference power constraint. This is due to the fact that the power control policy of SU is more flexible under the average over the peak interference power constraint.

Fig. 8 shows the outage probability for different fading models under the peak interference power constraint only with $r_0 = 1$ bit/complex dim.. It is observed that the simulation results match the analytical results very well. Moreover, it is observed that the outage probability curves overlap when Q_{pk} is very small, indicating that the fading models do not affect the outage probability notably for small value of Q_{pk}.

Fig. 9 illustrates the outage capacity versus average interference power constraint Q_{av} when the target rate r_0 is 1 bit/complex dim.. It is observed that the outage probability for Nakagami fading and log-normal shadowing drop sharply when Q_{av} reaches a certain value. This demonstrates that when Q_{av} approaches infinity, the outage probability becomes zero. In contrast, there is no such an evident threshold observed for Rayleigh fading channel, since its delay-limited capacity is zero. Additionally, comparing Fig.s 8 and 9, it is observed that the outage probability under average interference power constraint is smaller than that under peak interference power constraint when $Q_{av} = Q_{pk}$, suggesting that the power allocation scheme under the former is more flexible over the latter. Furthermore, comparing Fig. 9 with Fig. 5, it is observed that Q_{av} required to achieve the zero-outage probability for $r_0 = 1$ bit/complex dim. is consistent with that required to achieve the same delay-limited capacity.

VII. Conclusions

In this paper, the optimal power allocation strategies to achieve the ergodic, delay-limited, and outage capacities of a SU fading channel under spectrum sharing are studied, subject to different combinations of peak/average transmit and/or peak/average interference power constraints. It is shown that under the same threshold value, average interference power constraints are more flexible over their peak constraint counterparts to maximize SU fading channel capacities. The effects of different fading channel statistics on achievable SU capacities are also analyzed. One important observation made in this paper is that fading of the channel between SU-Tx and PU-Rx can be a good phenomenon for maximizing the capacity of SU fading channel.

Appendix A Proof of Theorem 1

By introducing the dual variable associated with the average interference power constraint, the partial Lagrangian of this problem is expressed as

$$L(P(g_0,g_1),\lambda) = \mathrm{E}\left[\log_2\left(1+\frac{g_1P(g_0,g_1)}{N_0}\right)\right] -\lambda\left(\mathrm{E}[g_0P(g_0,g_1)]-Q_{av}\right), \quad (48)$$

where λ is the nonnegative dual variable associated with the constraint $\mathrm{E}[g_0P(g_0,g_1)] \le Q_{av}$.

Let $\mathcal{A}$ denote the set of $\{0 \le P(g_0,g_1) \le P_{pk}\}$. The dual function is then expressed as

$$q(\lambda) = \max_{P(g_0,g_1)\in\mathcal{A}} L(P(g_0,g_1),\lambda). \quad (49)$$

The Lagrange dual problem is then defined as $\min_{\lambda\ge 0} q(\lambda)$. It can be verified that the duality gap is zero for the convex optimization problem addressed here, and thus solving its dual problem is equivalent to solving the original problem. Therefore, according to the Karush-Kuhn-Tucker (KKT) conditions [20], the optimal solutions needs to satisfy the following equations:

$$0 \le P(g_0,g_1) \le P_{pk}, \quad \mathrm{E}[g_0P(g_0,g_1)] \le Q_{av}, \quad (50)$$

$$\lambda(\mathrm{E}[g_0P(g_0,g_1)] - Q_{av}) = 0. \quad (51)$$

For a fixed λ, by dual decomposition [21], the dual function can be decomposed into a series of similar sub-dual-functions each for one fading state. For a particular fading state, the problem can be shown equivalent to

$$\max_{P(g_0,g_1)} \log_2\left(1+\frac{g_1P(g_0,g_1)}{N_0}\right) - \lambda g_0P(g_0,g_1), \quad (52)$$

$$\text{s.t.} \quad P(g_0,g_1) \le P_{pk}, \quad (53)$$

$$P(g_0,g_1) \ge 0. \quad (54)$$

The dual function of this sub-problem is

$$L_{sub}(P(g_0,g_1),\mu,\nu) = \log_2\left(1+\frac{g_1P(g_0,g_1)}{N_0}\right) - \lambda g_0P(g_0,g_1) -\mu(P(g_0,g_1)-P_{pk}) + \nu P(g_0,g_1), \quad (55)$$

where μ and ν are the nonnegative dual variables associated with the constraints (53) and (54), respectively.

The sub-dual problem is then defined as $q_{sub}(\mu,\nu) = \min_{\mu\ge 0,\nu\ge 0} L_{sub}(P(g_0,g_1),\mu,\nu)$. This is also a convex optimization problem for which the duality gap is zero. Therefore, according to the KKT conditions, the optimal solutions needs to satisfy the following equations:

$$\mu(P(g_0,g_1) - P_{pk}) = 0, \quad (56)$$

$$\nu P(g_0,g_1) = 0, \quad (57)$$

$$\frac{Kg_1}{g_1P(g_0,g_1)+N_0} - \lambda g_0 - \mu + \nu = 0. \quad (58)$$

From (58), it follows

$$P(g_0,g_1) = \frac{K}{\mu-\nu+\lambda g_0} - \frac{N_0}{g_1}. \quad (59)$$

Suppose that $P(g_0,g_1) < P_{pk}$, when $g_0 \le \frac{K}{\lambda(P_{pk}+\frac{N_0}{g_1})}$ or equivalently $(\frac{K}{\lambda g_0}-\frac{N_0}{g_1}) \ge P_{pk}$. Then, from (56), it follows that $\mu = 0$. Therefore, (59) reduces to $P(g_0,g_1) = \frac{K}{-\nu+\lambda g_0} - \frac{N_0}{g_1}$. Then $P(g_0,g_1) < P_{pk}$ results in $\frac{K}{-\nu+\lambda g_0} - \frac{N_0}{g_1} < P_{pk}$. Since $\nu \ge 0$, it follows that $P_{pk} > \frac{K}{-\nu+\lambda g_0} - \frac{N_0}{g_1} \ge \frac{K}{\lambda g_0} - \frac{N_0}{g_1}$. This contradicts the presumption. Therefore, from (50), it follows that

$$P(g_0,g_1) = P_{pk}, \quad \text{if} \quad g_0 \le \frac{K}{\lambda(P_{pk}+\frac{N_0}{g_1})}. \quad (60)$$

Suppose $P(g_0,g_1) > 0$, when $g_0 \ge \frac{Kg_1}{\lambda N_0}$ or equivalently $\frac{K}{\lambda g_0} - \frac{N_0}{g_1} \le 0$. Then, from (57), it follows that $\nu = 0$.

Therefore, (59) reduces to $P(g_0,g_1)=\frac{K}{\mu+\lambda g_0}-\frac{N_0}{g_1}$. Then $P(g_0,g_1)>0$ results in $\frac{K}{\mu+\lambda g_0}-\frac{N_0}{g_1}>0$. Since $\mu\geq 0$, it follows that $\frac{K}{\lambda g_0}-\frac{N_0}{g_1}\geq\frac{K}{\mu+\lambda g_0}-\frac{N_0}{g_1}>0$. This contradicts with the presumption. Therefore, from (50), it follows

$$P(g_0,g_1)=0,\quad \text{if}\quad g_0\geq\frac{Kg_1}{\lambda N_0}. \tag{61}$$

Suppose $P(g_0,g_1)=0$, when $\frac{Kg_1}{\lambda N_0}>g_0>\frac{K}{\lambda(P_{pk}+\frac{N_0}{g_1})}$ or equivalently $0<\frac{K}{\lambda g_0}-\frac{N_0}{g_1}<P_{pk}$. Then, from (56), it follows that $\mu=0$. Therefore, (59) reduces to $P(g_0,g_1)=\frac{K}{-\nu+\lambda g_0}-\frac{N_0}{g_1}$. Then $P(g_0,g_1)=0$ results in $\frac{K}{-\nu+\lambda g_0}-\frac{N_0}{g_1}=0$. Since $\nu\geq 0$, it follows that $0>\frac{K}{-\nu+\lambda g_0}-\frac{N_0}{g_1}\geq\frac{K}{\lambda g_0}-\frac{N_0}{g_1}$. This contradicts the presumption. Therefore, $P(g_0,g_1)\neq 0$ for this set of g_0. Next, suppose $P(g_0,g_1)=P_{pk}$ for the same set of g_0. Then, from (57), it follows that $\nu=0$. Therefore, (59) reduces to $P(g_0,g_1)=\frac{K}{\mu+\lambda g_0}-\frac{N_0}{g_1}$. Then $P(g_0,g_1)=P_{pk}$ indicates $\frac{K}{\mu+\lambda g_0}-\frac{N_0}{g_1}=P_{pk}$. Since $\mu\geq 0$, it follows $\frac{K}{\lambda g_0}-\frac{N_0}{g_1}\geq\frac{K}{\mu+\lambda g_0}-\frac{N_0}{g_1}=P_{pk}$. This contradicts the presumption. Therefore, $P(g_0,g_1)\neq P_{pk}$ for this set of g_0. Now, from (57), $P(g_0,g_1)\neq 0$ results in $\nu=0$. From (56), $P(g_0,g_1)\neq P_{pk}$ results in $\mu=0$. Therefore, from (59), it follows

$$P(g_0,g_1)=\frac{K}{\lambda g_0}-\frac{N_0}{g_1},\quad \text{if}\quad \frac{Kg_1}{\lambda N_0}>g_0>\frac{K}{\lambda(P_{pk}+\frac{N_0}{g_1})}. \tag{62}$$

From (51), it is easy to observe that λ is either equal to zero or determined by solving $\mathrm{E}[g_0P(g_0,g_1)]=Q_{av}$.

Theorem 1 is thus proved.

APPENDIX B
PROOF OF THEOREM 3

The proof is organized in two steps. First, we show that the solution of (23) subject to $\mathscr{F}_2$ must have the same structure as (26). Secondly, we show that λ is determined by substituting (26) into the constraint $\mathrm{E}\left[g_0P(g_0,g_1)\right]=Q_{av}$.

Step 1: Define an indicator function,

$$\chi=\begin{cases}1, & \log_2\left(1+\frac{g_1P(g_0,g_1)}{N_0}\right)<r_0\\ 0, & \text{otherwise}\end{cases}. \tag{63}$$

Then the optimization problem (23) subject to $\mathscr{F}_2$ can be rewritten as

$$\min_{P(g_0,g_1)\in\mathscr{F}_2}\mathrm{E}\left\{\chi\right\}. \tag{64}$$

By introducing the dual variable λ associated with the average interference power constraint, the partial Lagrangian of this problem is expressed as

$$L\left(P(g_0,g_1),\lambda\right)=\mathrm{E}\left\{\chi\right\}+\lambda\left(\mathrm{E}\{g_0P(g_0,g_1)\}-Q_{av}\right). \tag{65}$$

Let $\mathcal{A}$ denote the set of $\{P(g_0,g_1):0\leq P(g_0,g_1)\leq P_{pk}\}$. The dual function is then expressed as

$$\min_{P(g_0,g_1)\in\mathcal{A}}\mathrm{E}\left\{\chi\right\}+\lambda\left(\mathrm{E}\{g_0P(g_0,g_1)\}-Q_{av}\right). \tag{66}$$

For a fixed λ, by dual decomposition, the dual function can be decomposed into a series of similar sub-dual-functions each for one fading state. For a particular fading state, the problem can be shown equivalent to

$$\min_{P(g_0,g_1)}\quad \chi+\lambda g_0P(g_0,g_1), \tag{67}$$

$$\text{s.t.}\quad P(g_0,g_1)\leq P_{pk}, \tag{68}$$

$$P(g_0,g_1)\geq 0. \tag{69}$$

When $\chi=1$, (67) is minimized if $P(g_0,g_1)=0$, and the minimum value of (67) is 1; when $\chi=0$, (67) is minimized if $P(g_0,g_1)=\frac{N_0(2^{r_0}-1)}{g_1}$, and the minimum value of (67) is $\lambda g_0\frac{N_0(2^{r_0}-1)}{g_1}$. Thus, $P(g_0,g_1)=\frac{N_0(2^{r_0}-1)}{g_1}$ is the optimal solution of the problem, only when $\lambda g_0\frac{N_0(2^{r_0}-1)}{g_1}<1$ and $\frac{N_0(2^{r_0}-1)}{g_1}\leq P_{pk}$ are satisfied simultaneously. Otherwise, $P(g_0,g_1)=0$ is the optimal solution of the problem. Therefore, the optimal solution has the same structure as (26).

Step 2: Suppose $P^*(g_0,g_1)$ is the optimal solution of (23) subject to $\mathscr{F}_2$ with $\lambda=\lambda^*>0$ satisfying $\mathrm{E}\left[g_0P^*(g_0,g_1)\right]<Q_{av}$. Suppose $P'(g_0,g_1)$ is a solution of (23) subject to $\mathscr{F}_2$ with $\lambda=\lambda'>0$, which satisfies $\mathrm{E}\left[g_0P'(g_0,g_1)\right]=Q_{av}$. Then, it is easy to verify that $\lambda^*>\lambda'$. Therefore, from (27), it follows

$$\mathscr{P}^*_{out}>\mathscr{P}'_{out} \tag{70}$$

where the inequality results from the fact that $\lambda^*>\lambda'$ and $\mathscr{P}_{out}$ is an increasing function with respect to λ. This result contradicts our presumption. Therefore, the optimal λ must be determined by solving $\mathrm{E}\left[g_0P(g_0,g_1)\right]=Q_{av}$. Otherwise, if $\lambda=0$, the power allocation strategy obtained in step 1 reduces to the truncated channel inversion given in [6], and this holds only when $\mathrm{E}\left[g_0P(g_0,g_1)\right]<Q_{av}$.

Theorem 3 is thus proved.

REFERENCES

[1] "Spectrum policy task force," Federal Communications Commission, ET Docket No. 02-135, Tech. Rep., Nov. 2002.

[2] J. Mitola and G. Q. Maguire, "Cognitive radio: making software radios more personal," *IEEE Pers. Commun.*, vol. 6, no. 6, pp. 13-18, Aug. 1999.

[3] S. Haykin, "Cognitive radio: brain-empowered wireless communications," *IEEE J. Select. Areas Commun.*, vol. 23, no. 2, pp. 201-220, Feb. 2005.

[4] Y.-C. Liang, Y. Zeng, E. C. Y. Peh, and A. T. Hoang, "Sensing-throughput tradeoff for cognitive radio networks," *IEEE Trans. Wireless Commun.*, vol. 7, no. 4, pp. 1326-1337, Apr. 2008.

[5] A. Ghasemi and E. S. Sousa, "Fundamental limits of spectrum-sharing in fading environments," *IEEE Trans. Wireless Commun.*, vol. 6, no. 2, pp. 649-658, Feb. 2007.

[6] A. J. Goldsmith and P. P. Varaiya, "Capacity of fading channels with channel side information," *IEEE Trans. Inform. Theory*, vol. 43, no. 6, pp. 1986-1992, Nov. 1997.

[7] E. Biglieri, J. Proakis, and S. Shamai, "Fading channels: information-theoretic and communications aspects," *IEEE Trans. Inform. Theory*, vol. 44, no. 6, pp. 2619-2692, Oct. 1998.

[8] Y.-C. Liang, R. Zhang, and J. Cioffi, "Subchannel grouping and statistical waterfilling for vector block-fading channels," *IEEE Trans. Commun.*, vol. 54, no. 6, pp. 1131-1142, June 2006.

[9] M. Gastpar, "On capacity under receive and spatial spectrum-sharing constraints," *IEEE Trans. Inform. Theory*, vol. 53, no. 2, pp. 471-487, Feb. 2007.

[10] L. Musavian and S. Aissa, "Ergodic and outage capacities of spectrum-sharing systems in fading channels," in *Proc. IEEE Global Telecommunications Conference (GLOBECOM'07)*, Washington. DC, USA, 2007, pp. 3327-3331.

[11] R. Zhang and Y.-C. Liang, "Exploiting multi-antennas for opportunistic spectrum sharing in cognitive radio networks," *IEEE J. Select. Topics Signal Processing*, vol. 2, no. 1, pp. 1-14, Feb. 2008.

[12] L. Zhang, Y.-C. Liang, and Y. Xin, "Joint beamforming and power allocation for multiple access channels in cognitive radio networks," *IEEE J. Select. Areas Commun.*, vol. 26, no. 1, pp. 38-51, Jan. 2008.
[13] L. Ozarow, S. Shamai, and A. D. Wyner, "Information theoretic considerations for cellular mobile radio," *IEEE Trans. Veh. Technol.*, vol. 43, pp. 359-378, May 1994.
[14] G. Caire, G. Taricco, and E. Biglieri, "Optimum power control over fading channels," *IEEE Trans. Inform. Theory*, vol. 45, no. 5, pp. 1468-1489, July 1999.
[15] S. V. Hanly and D. N. Tse, "Multi-access fading channels-part ii: delay-limited capacities," *IEEE Trans. Inform. Theory*, vol. 44, no. 7, pp. 2816-2831, Nov. 1998.
[16] M. Khojastepour and B. Aazhang, "The capacity of average and peak power constrained fading channels with channel side information," in *Proc. IEEE Wireless Commun. Networking Conf.*, vol. 1, Mar. 2004, pp. 77-82.
[17] I. S. Gradshteyn and I. M. Ryzhik, *Table of Integrals, Series, and Products*, 5th ed. San Diego: Academic Press, 1994.
[18] M. Nakagami, "The m-distribution, a general formula of intensity distribution of rapid fading," in *Statistical Methods in Radio Wave Propagatio*, W. G. Hoffman, Ed. Oxford, England: Pergamon, 1960.
[19] A. Papoulis and S. U. Pillai, *Probability, Random Variables and Stochastic Processes*. New York: McGraw Hill Higher Education, 2002.
[20] S. Boyd and L. Vandenberghe, *Convex Optimization*. Cambridge, UK: Cambridge University Press, 2004.
[21] R. Zhang, S. Cui, and Y.-C. Liang, "On ergodic sum capacity of fading cognitive multiple-access and broadcast channels," submitted to *IEEE Trans. Inform. Theory* (also available at arXiv: 0806.4468).

Xin Kang (S'08) received his B.Sc. degree in Electrical Engineering from the Xi'an Jiao Tong University, China, in 2005. He is currently working toward his Ph.D. degree in the Electrical and Computer Engineering Department at the National University of Singapore. His research interests include cognitive radio networks, multiuser communication systems and power allocation for fading channels.

Ying-Chang Liang (SM'00) is now Senior Scientist in the Institute for Infocomm Research (I2R), Singapore, where he has been leading the research activities in the area of cognitive radio and cooperative communications and the standardization activities in IEEE 802.22 wireless regional networks (WRAN) for which his team has made fundamental contributions in physical layer, MAC layer and spectrum sensing solutions. He also holds adjunct associate professorship positions in Nanyang Technological University (NTU) and National University of Singapore (NUS), both in Singapore, and adjunct professorship position in University of Electronic Science and Technology of China (UESTC). He has been teaching graduate courses in NUS since 2004. From Dec 2002 to Dec 2003, he was a visiting scholar with the Department of Electrical Engineering, Stanford University. His research interest includes cognitive radio, dynamic spectrum access, reconfigurable signal processing for broadband communications, space-time wireless communications, wireless networking, information theory and statistical signal processing.

He is now an Associate Editor of IEEE TRANSACTIONS ON VEHICULAR TECHNOLOGY. He served as an Associate Editor of IEEE TRANSACTIONS ON WIRELESS COMMUNICATIONS from 2002 to 2005, Lead Guest-Editor of IEEE JOURNAL ON SELECTED AREAS IN COMMUNICATIONS, Special Issue on Cognitive Radio: Theory and Applications, and Guest-Editor of COMPUTER NETWORKS JOURNAL (Elsevier) Special Issue on Cognitive Wireless Networks. He received the Best Paper Awards from IEEE VTC-Fall'1999 and IEEE PIMRC'2005, and 2007 Institute of Engineers Singapore (IES) Prestigious Engineering Achievement Award.

Arumugam Nallanathan (S'97−M'00−SM'05) received the B.Sc. with honors from the University of Peradeniya, Sri-Lanka, in 1991, the CPGS from the Cambridge University, United Kingdom, in 1994 and the Ph.D. from the University of Hong Kong, Hong Kong, in 2000, all in Electrical Engineering. He was an Assistant Professor in the Department of Electrical and Computer Engineering, National University of Singapore, Singapore from August 2000 to December 2007. Currently, he is a Senior Lecturer in the Department of Electronic Engineering at King's College London, United Kingdom. His research interests include cooperative communications, cognitive radio, MIMO-OFDM systems, ultra-wide bandwidth (UWB) communication and localization. In these areas, he has published over 130 journal and conference papers. He is a co-recipient of the Best Paper Award presented at 2007 IEEE International Conference on Ultra-Wideband (ICUWB'2007).

He currently serves on the Editorial Board of IEEE TRANSACTIONS ON WIRELESS COMMUNICATIONS and IEEE TRANSACTIONS ON VEHICULAR TECHNOLOGY as an Associate Editor. He served as a Guest Editor for EURASIP JOURNAL OF WIRELESS COMMUNICATIONS AND NETWORKING: Special issue on UWB Communication Systems–Technology and Applications. He served as a technical program committee member for more than 30 IEEE international conferences. He also served as the General Track Chair for the IEEE VTC'2008-Spring. He currently serves as the Co-Chair for the IEEE GLOBECOM'2008 Signal Processing for Communications Symposium, and IEEE ICC'2009 Wireless Communications Symposium.

Hari Krishna Garg received the B.Tech. degree from the Indian Institute of Technology (IIT), Delhi, the M.Eng. and Ph.D. degrees from Concordia University, Montreal, QC, Canada, and the MBA degree from Syracuse University, Syracuse, NY, USA.

He has been a faculty member of the Electrical and Computer Engineering Department at Syracuse University. Currently, he is with the Electrical and Computer Engineering Department at National University of Singapore. His research area of interest is mobile communications from the physical layer to the applications on both technology as well as applications' front. More recently, he has been active as entrepreneur having founded or co-founded four companies.

Rui Zhang (S'00-M'07) received the B.S. and M.S. degrees in electrical and computer engineering from National University of Singapore in 2000 and 2001, respectively, and the Ph.D. degree in electrical engineering from Stanford University, Stanford, CA, in 2007. Since 2007, he has been a Research Fellow with the Institute for Infocomm Research (I2R), A*STAR, Singapore. His recent research interests include cognitive radio networks, cooperative communication systems, and multiuser MIMO transmission systems.